Formation and electrical evaluation of a single metallized DNA nanowire in a nanochannel

Takahiro Himuro,[a] *Shinobu Sato,*[b] *Shigeori Takenaka,*[b] *Takashi Yasuda* [a]*

[a] Graduate School of Life Science and Systems Engineering, Kyushu Institute of Technology
[b] Graduate School of Engineering, Kyushu Institute of Technology
* e-mail: yasuda@life.kyutech.ac.jp

Received: ((will be filled in by the editorial sttaff))
Accepted: ((will be filled in by the editorial sttaff))

Abstract
A novel fabrication process was developed for a single silver nanowire using DNA metallization in a nanochannel, and the electrical properties of this nanowire were evaluated using electrochemical impedance spectroscopy. After being isolated using a nanochannel measuring 500 nm in depth and 500 nm in width, a single λDNA molecule was electrostatically stretched and immobilized between two electrodes separated by a gap of 15 μm by applying an AC voltage of 1 MHz and 20 $V_{p\text{-}p}$. Then, naphthalene diimide molecules terminally-labeled with galactose moieties were intercalated into the λDNA, and the reduction of silver ions along the λDNA led to its metallization with silver. Scanning electron microscopy observations revealed that two nanowires having different average widths of 154 nm and 250 nm were formed in two individual nanochannels. The nanowires showed the linear current-voltage characteristics, and their combined resistance was estimated to be 45.5 Ω. The complex impedance of the nanowires was measured, and an equivalent circuit was obtained as a series connection of a resistance and a parallel resistance-constant phase element circuit. Impedance analysis revealed that the nanowire included silver grain boundaries, and the bulk resistivity of silver grain was estimated to be 8.35×10^{-8} Ωm.

Keywords: DNA, Metallization, Nanowire, Nanochannel, Impedance spectroscopy

DOI: 10.1002/elan.((will be filled in by the editorial sttaff))

1. Introduction

DNA-based nanotechnology has advanced to the point where various nanostructures can be built by self-assembly of designed DNA molecules. This technology is expected to find application in a variety of fields, such as electronics and medicine [1-2]. Also, the DNA molecule is one of the strongest candidates for nanoscale electronic components [3-7]. However, the use of DNA as a conductive nanowire is difficult because the DNA molecule has a high electrical resistance that varies unstably depending on the DNA base sequence and ambient conditions [6]. One solution to this problem is to metallize DNA molecules through the deposition of metal atoms. Numerous research groups have already reported metallized DNA nanowires [8-30]. The most common method for DNA metallization is electroless plating through the reduction of metal ions that are electrostatically bound to negatively-charged DNA strands [9-20]. Also, Fischler *et al*. preliminarily modified DNA with reducing sugar and metallized the DNA by the reduction of metal ions [25]. Then, Al-Said *et al*. formed uniform conductive nanowires by metallizing DNA/conducting polymer hybrid nanowires [29]. Moreover, we intercalated galactose-modified naphthalene diimides into a double-stranded DNA and reduced metal ions on the DNA surfaces [30].

In order to apply a metallized DNA nanowire to an electronic component, it is very important to immobilize a single nanowire between two electrodes and determine the details of its electrical properties. Several research groups have already carried out an electrical assessment of metallized DNA nanowires. Pearson *et al*. placed a nanowire-containing droplet over electrodes and measured the electrical resistance of nanowires that bridged an electrode gap by chance [28]. In this method, it is difficult to control the number of nanowires immobilized between the electrodes. Moreover, the high contact resistance between the nanowires and electrodes decreases the measurement precision. Ijiro *et al*. stretched and immobilized DNA molecules on a glass substrate

using the Langmuir-Blodgett (LB) method before metallization and measured the conductivity of the nanowire by placing the probe of a conductive atomic force microscope (AFM) into contact with one end of the nanowire, with the other end immobilized on an electrode [24]. The problem with this method is that the contact resistance changes unpredictably depending on the contact force between the nanowire and AFM probe tip. Braun *et al*. stretched DNA molecules by fluid flow or electrophoresis, hybridized them with oligonucleotides preliminarily bound to two electrodes, and then performed DNA metallization [10]. This method permits a low stable contact resistance at the electrode-nanowire interface, but requires complicated pretreatments, such as functionalization of DNA molecules and modification of electrode surfaces. Moreover, it does not guarantee the electrical measurement of a single nanowire because it involves no isolation of a single DNA molecule.

Nanochannels have recently received extensive attention in nanobiotechnology because they are powerful tools for manipulating and analyzing biomolecules such as DNA at the single-molecule level [31-34]. In the present study, in order to isolate a single DNA molecule, we used a nanochannel that is shallower and narrower than the radius of gyration of a DNA molecule. Also, we electrostatically stretched and immobilized a DNA molecule between two electrodes in a nanochannel by applying an alternating electric field [35-36]. This permitted simple, highly reproducible stretching and immobilization of a single DNA molecule without any DNA pretreatment or electrode surface modification. Then, by using intercalator molecules (naphthalene diimides) terminally-labeled with reducing groups (galactoses), we metallized a DNA molecule and formed a single nanowire in a nanochannel. Moreover, for the first time, we determined the impedance frequency characteristics of a nanowire and derived its equivalent circuit.

2. Materials and methods

2.1. Nanowire formation

A device for nanowire formation consists of a microchannel, a nanochannel, and two gold electrodes (Fig. 1). The nanochannel branches orthogonally from the microchannel, and the electrode surfaces are partially exposed inside the nanochannel. When a 100 μl of solution containing λDNA (Takara Bio Inc.) was injected into the microchannel using a syringe pump (Fig. 1(a)), a single λDNA molecule was introduced into a nanochannel by capillary force (Fig. 1(b)). To prevent two or more λDNA molecules from invading a nanochannel, the λDNA solution was preliminarily diluted to a low concentration of 1 nM with ultrapure water (Milli-Q water, Merck Millipore Corp.). Then, the application of an AC voltage of 1 MHz and 20 V_{p-p} stretched and immobilized the λDNA molecule between the electrodes (Fig. 1(c)). The amplitude and frequency of the applied voltage were controlled using a function generator (FGX-295, TEXIO Technology Corp.) and a high-speed bipolar amplifier (HSA4101, NF Corp.). The voltage waveforms were monitored by an oscilloscope (TDS 3014, Tektronix, Inc.). Also, λDNA molecules preliminarily labeled with the fluorescence dye Hoechst 33258 (Takara Bio Inc.) were observed with an upright fluorescence microscope (MZ16 F-FluoCombi III, Leica Microsystems K.K.). The molecular behavior was monitored using a CMOS camera (ORCA-Flash 4.0, Hamamatsu Photonics K.K.), and analyzed by the HCImage Live Software (Hamamatsu Photonics K.K.).

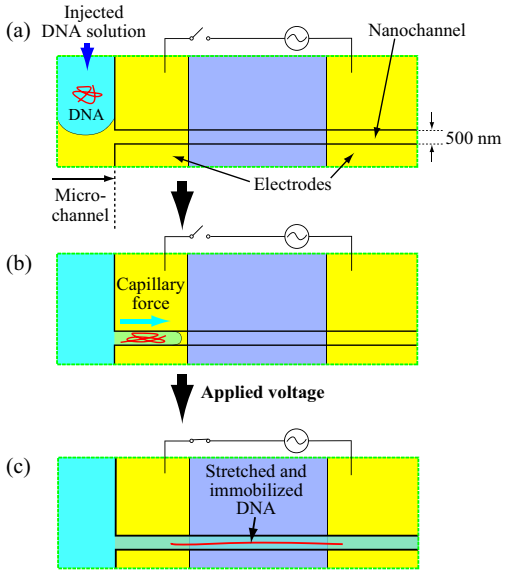

Fig. 1. Procedure for isolation of a single DNA molecule in a nanochannel and stretch/immobilization of the DNA between two electrodes. (a) Injection of a DNA solution into a microchannel. (b) Transport of a single DNA molecule into a nanochannel by capillary force. (c) Electrostatic stretch and immobilization of the DNA by an applied AC voltage of 1 MHz and 20 V_{p-p} between two electrodes placed 15 μm apart in the nanochannel.

Naphthalene diimide (NDI) terminally-labeled with two galactose moieties (abbreviated as NDI-DS2) (Fig. 2(a)) was used for DNA metallization [30]. NDI

molecules act as threading intercalators, forming a stable complex with a double-stranded DNA. Then, the galactose moieties act as reducing agents. NDI-DS2 was synthesized by the click reaction of the acetylene derivative of NDI with galactose azide. When a 100 µl of 20 nM NDI-DS2 solution was introduced into the microchannel using a syringe pump, the NDI-DS2 molecules diffused into the nanochannel and were intercalated into the double strand of λDNA so that the galactoses were arranged along the λDNA. In order to allow sufficient time for the diffusion and intercalation of NDI-DS2, we let the solution stand still in the microchannel for 30 min. After that, the channels were rinsed for 30 min by replacing the solution with ultrapure water in order to remove unbound NDI-DS2 molecules. Then, when a 100 µl of 0.1 M Tollens' reagent containing silver ions was injected into the microchannel, silver ions diffused into the nanochannel, and the λDNA was metallized with silver because the galactose moieties reduced silver ions along the λDNA (Fig. 2(b)). After the Tollens' reagent was held in the microchannel for 5 h, the channels were rinsed four times by replacing the solution with ultrapure water and holding it in the microchannel for 15 min during each rinse.

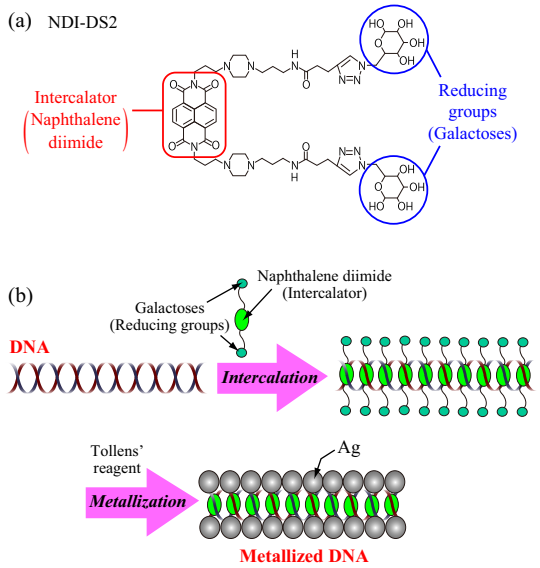

Fig. 2. Materials and methods used for λDNA metallization. (a) Structural formula of naphthalene diimide (NDI) terminally-labeled with two galactose moieties (referred to as NDI-DS2). NDI molecules act as threading intercalators that form a stable complex with a double-stranded DNA. The galactose moieties act as reducing agents. (b) Procedure for metallization of a single DNA molecule. NDI-DS2 molecules are intercalated into the double strand of λDNA so that the galactoses are arranged along the λDNA. When a Tollens' reagent containing silver ions is injected, the λDNA is metallized with silver because the galactose moieties reduce silver ions along the λDNA.

2.2. Device design and fabrication

The schematics and photographs of a micro/nano-fluidic device for nanowire formation are shown in Figs. S1 and S2, respectively. Because the concentration of the λDNA solution was low enough for the isolation of a single λDNA in a nanochannel, the probability of the invasion of the nanochannel by a single λDNA was lower than about 10%. Therefore, in order to increase the success rate of capturing a single λDNA in a nanochannel, we arranged 15 parallel nanochannels connected to a microchannel on a device. As described below in detail, the nanochannels and two electrodes were fabricated on a Si wafer. Then, a microchannel measuring 50 µm in depth, 500 µm in width, and 10 mm in length was fabricated by polydimethylsiloxane (PDMS) molding and mounted on the nanochannels and electrodes. The nanochannel was designed to be 500 nm deep, 500 nm wide, and 100 µm long because the radius of gyration of the λDNA was estimated to be about 520 nm [37]. Also, the nanochannel fabricated by focused ion beam (FIB) etching had a cross-section shaped like an inverted triangle, probably because the ion beam had a Gaussian distribution [38]. The two gold electrodes were patterned after the wafer surface was insulated by thermal oxidation. In order to immobilize both ends of the λDNA between the electrodes, we set the electrode gap to be 15 µm, which is slightly shorter than the λDNA length of 16 µm.

The nanochannels and electrodes were fabricated on a silicon wafer as follows (Fig. S3). First, $500^{w}\times500^{d}$ nm nanochannels were fabricated by etching the wafer using an FIB system (JFIB-2300, JEOL Ltd.). Then, the wafer surface was thermally oxidized, resulting in the formation of a 200-nm-thick SiO_2 layer. After that, the wafer was spin-coated with a ZPN-1150 photoresist (ZEON Corp.), and the photoresist was patterned using UV lithography. Next, a roughly 100-nm-thick Au layer with an approximately 30-nm-thick adhesive Cr layer was deposited by vacuum evaporation (VPC-260, ULVAC Kiko, Inc.), and the electrodes were patterned by a lift-off process. On the other hand, the microchannel was made of PDMS (KE106, Shin-Etsu Chemical Co., Ltd.). A 50-µm-thick layer of SU-8 3050 photoresist (Nippon Kayaku Co., Ltd) was patterned on another Si wafer to serve as a mold for the microchannel. Then, a mixture of liquid PDMS and cross-linking agent (CAT-RG, Nippon Kayaku Co., Ltd) was cast over the SU-8 mold, which had two rivets inserted into inlet/outlet tubes. After the PDMS was cured in a furnace, the PDMS plate with the microchannel was peeled from the mold. Finally, the PDMS plate was bonded to the Si wafer over the nanochannels and electrodes after their surfaces were

hydrophilized with O_2 plasma treatment in order to improve their wettability.

2.3. Electrical evaluation

In order to obtain a value of DC resistance of the fabricated nanowire, a current-voltage characteristic was evaluated using an electrochemical analyzer (ALS802B, BAS Inc.). The working electrode of the analyzer was connected to one of the two electrodes on the device, and the counter and reference electrodes were connected to the other electrode. Then, a current between the two electrodes was measured while sweeping an applied DC voltage from 0 V to 0.1 V.

Next, in order to reveal the detailed electrical properties such as bulk resistance, parasitic resistance, and parasitic capacitance which are attributed to silver grains and their boundaries composing the nanowire, we evaluated the impedance frequency characteristics of the nanowire using electrochemical impedance spectroscopy (EIS). While sweeping the voltage frequency from 4 Hz to 5 MHz, the complex impedance between the electrodes in ultrapure water was measured using an impedance analyzer (IM3570, Hioki E.E. Corp.). Then, the measured impedance spectrum was plotted on the complex plane, and an equivalent circuit of the nanowire was obtained by precisely fitting a complex impedance plot of the circuit model to that of the nanowire. This revealed the composition of electrical components of the nanowire.

3. Results and discussion

3.1. Nanowire formation

In order to check the isolation of a single λDNA in the nanochannel and its stretch/immobilization between the electrodes, we observed a λDNA that was preliminarily labeled with Hoechst 33258. Thus, a fluorescence image of the λDNA stretched and immobilized between the electrodes in the nanochannel was obtained (see Fig. 3). Also, the λDNA was found to retain its stretched and immobilized state even after voltage application was terminated. In these observations, the roughly 5-mm-thick PDMS microchannel plate was removed from the device because it strongly interfered with the fluorescence imaging. Moreover, the reflection of an excitation light on the electrodes generated intense background fluorescence, which made the imaging of λDNA motion more difficult.

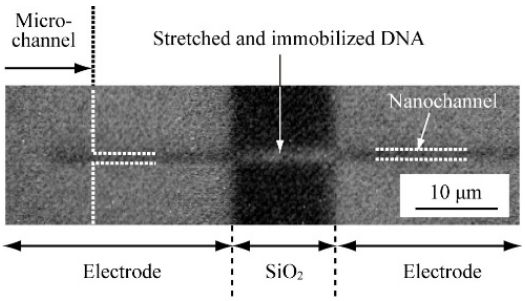

Fig. 3. Fluorescence image of the λDNA, stretched and immobilized between the two electrodes in the nanochannel. The λDNA was preliminarily labeled with the fluorescence dye Hoechst 33258. Here, the PDMS microchannel plate was removed from the device because it strongly interfered with the fluorescence imaging.

After several experiments, we succeeded in forming a single silver nanowire in each of two nanochannels on a single device with 15 nanochannels in total. The scanning electron microscope (SEM) images of the nanowire are shown in Fig. 4. The nanowire width was measured for every 500 nm length from the SEM images. One of the nanowires had an average width of 154 nm and a standard deviation of 62.2 nm (Fig. 4(a)). The other nanowire had an average width of 250 nm and a standard deviation of 21.1 nm (Fig. 4(b)). A large variety of width of the two nanowires was probably due to a difference between concentrations of silver ions in the two nanochannels. While the Tollens' reagent was held in the microchannel for 5 h, the solutions in the nanochannels evaporated from their outlets because the outlets were open to the atmosphere. Different evaporation rates probably caused a large variety of concentrations of silver ions in the nanochannels.

The energy dispersive X-ray (EDX) analysis spectrum, which was obtained by focusing an electron beam onto the nanowire surface, demonstrated that the nanowire was made of Ag. In addition, Si, O, and C peaks were observed. The Si and O peaks originated from the device materials, while the C peak was attributed to the λDNA component and surface-adsorbed carbon (Fig. S4).

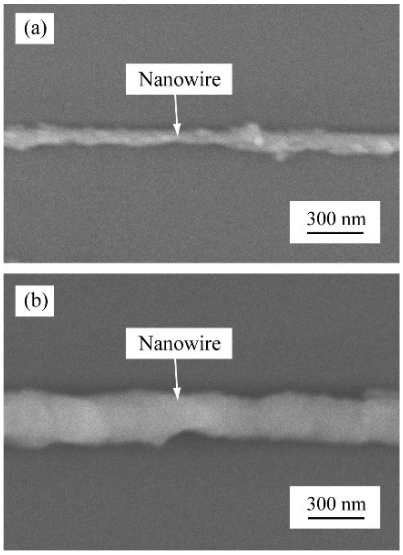

Fig. 4. SEM images of the single nanowires formed using λDNA metallization in the two nanochannels. (a) One of the nanowires had a width of 154 nm ± 62.2 nm. (b) The other nanowire had a width of 250 nm ± 21.1 nm.

3.2. Electrical evaluation

As shown in Fig. 5, the current-voltage characteristics of the two parallel nanowires which was obtained by applying a DC voltage between the two electrodes showed a linear ohmic behavior in the range of 0 to 0.1 V. The combined resistance of the nanowires was estimated to be 45.5 Ω. The nanowires had markedly higher conductivity than the previously-reported metallized DNA nanowires [28].

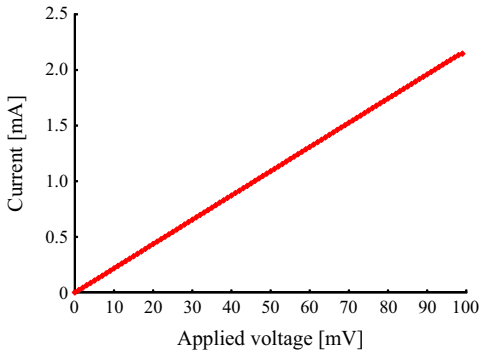

Fig. 5. Current-voltage characteristics of the two parallel nanowires. The nanowires showed a typical ohmic behavior, and their combined resistance was 45.5 Ω.

Figure 6 shows the impedance spectrum between the two electrodes that were connected with the two parallel nanowires. This spectrum clearly shows the frequency dependence of the nanowire impedance. The real part of the impedance at low frequencies (< 100 kHz), which was almost independent of frequency, was attributed to the resistive components of the nanowire. On the other hand, in the frequency range between 100 kHz and 1 MHz, the real part of the impedance decreased dramatically with increasing frequency, while its imaginary part showed a maximum at about 500 kHz. These results indicated that the nanowire incorporated capacitive components.

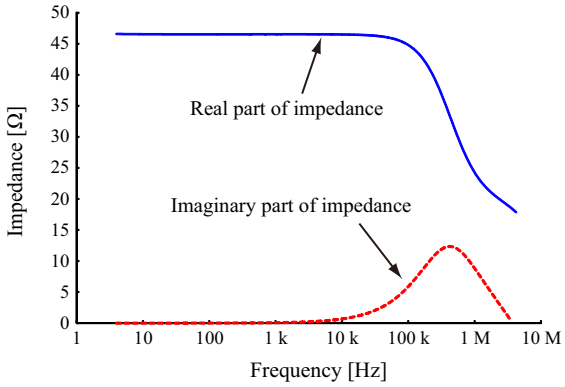

Fig. 6. Impedance spectrum between the two electrodes connected by the two parallel nanowires. The constant real part of the impedance at low frequencies is attributed to the resistive components of the nanowire. The dramatic changes of the real part and imaginary part in high frequencies indicate that the nanowire incorporates capacitive components.

The solid red line in Fig. 7(a) represents the complex impedance obtained from the above results over the frequency range of 4 Hz to 5 MHz. The semicircular shape of the plot suggests that the nanowire consisted of nearly homogeneous resistive and capacitive components, and that its equivalent circuit included a parallel resistance-capacitance (RC) circuit. Also, the smaller intercept where the semicircle crosses the real axis in the higher-frequency region has a positive value, which means that the equivalent circuit included a serial resistance component. Therefore, we assumed the equivalent circuit of the nanowire to be a series connection of a resistance, R_b, and a parallel RC circuit consisting of R_c and C (Fig. 7(b)). The complex impedance, Z, of the equivalent circuit is given by

$$Z = R_b + \frac{1}{\frac{1}{R_c} + j\omega C}, \qquad (1)$$

where j is the imaginary unit and ω is the angular frequency. We adjusted the values of three components, *viz.*, R_b, R_c, and C, so that the complex impedance plot of

the equivalent circuit would fit that of the nanowire. As a result, the fitting curve represented by the dashed-dotted black line in Fig. 7(a), which has the same intercepts as the complex impedance plot of the nanowire, was obtained using the component values listed in Table 1.

However, the above fitting analysis is inadequate because the two semicircles do not coincide perfectly. The center of the semicircle representing the parallel RC circuit is located on the real axis, but that of the semicircle for the nanowire shifted below the real axis. This is probably because the resistive and capacitive components of the nanowire were not entirely homogeneous, but rather, showed a slight variability. In order to obtain a better curve fit, we replaced the capacitance, C, with the constant phase element (CPE), Z_{CPE} (Fig. 7(c)). The CPE is a circuit element used to represent non-ideal capacitive interfacial behaviors that cannot be adequately understood by a simple capacitance element [39-41]. The impedance of CPE is described by

$$Z_{\mathrm{CPE}} = \frac{1}{X(j\omega)^{p}} \quad , \tag{2}$$

where X is the CPE coefficient with units of $\Omega^{-1}s^{p}$ and p is the CPE exponent that takes values between 0 and 1. In the cases of $p = 0$ and $p = 1$, CPE is equivalent to an ideal resistance and ideal capacitance, respectively. Therefore, the complex impedance of the equivalent circuit is modified as follows:

$$Z = R_{\mathrm{b}} + \frac{1}{\frac{1}{R_{\mathrm{c}}} + X(j\omega)^{p}} \tag{3}$$

$$\mathrm{Re}(Z) = R_{\mathrm{b}} + \frac{1 + R_{\mathrm{C}} X\omega^{p} \cos\frac{p\pi}{2}}{1 + 2R_{\mathrm{C}} X\omega^{p} \cos\frac{p\pi}{2} + (R_{\mathrm{C}} X\omega^{p})^{2}} R_{\mathrm{C}} \tag{4}$$

$$\mathrm{Im}(Z) = \frac{R_{\mathrm{C}} X\omega^{p} \sin\frac{p\pi}{2}}{1 + 2R_{\mathrm{C}} X\omega^{p} \cos\frac{p\pi}{2} + (R_{\mathrm{C}} X\omega^{p})^{2}} R_{\mathrm{C}} \quad . \tag{5}$$

The dashed blue line in Fig. 7(a) is the curve fit obtained by using the R-CPE circuit model and the parameter values listed in Table 1. Clearly, the R-CPE circuit model represents the electrical properties of the fabricated nanowire more precisely than the simple RC circuit model.

The presence of the capacitive component CPE, Z_{CPE}, suggests that the nanowire contains silver grain boundaries [42]. Then, the resistive component, R_c, which corresponds to the diameter of the semicircle, presumably represents the contact resistance at the grain boundaries. On the other hand, the serial resistive component, R_b, which corresponds to the intercept of the semicircle at the higher frequency, represents the total bulk resistance of the silver grains. In this case, the total bulk resistance, R_b, of the two parallel nanowires is 18.5 Ω. When the two nanowires are assumed to be solid cylinders which were made of silver without grain boundaries and have the same length, L, and different diameters, W_1 and W_2, the resistivity of silver, ρ, is given by

$$\rho = \frac{\pi R_{\mathrm{b}} \left(W_1^{2} + W_2^{2} \right)}{4L} \quad . \tag{6}$$

The substitutions R_b = 18.5 Ω, L = 15 μm (the electrode gap), W_1 = 154 nm, and W_2 = 250 nm give $\rho = 8.35\times10^{-8}$ Ωm. This value is larger than the bulk resistivity of pure silver (1.59×10^{-8} Ωm), but is two orders of magnitude smaller than that of the previously-reported metallized DNA nanowires [28]. Also, the bulk resistances of the two nanowires were calculated to be 67.2 Ω and 25.5 Ω using the value of resistivity, ρ.

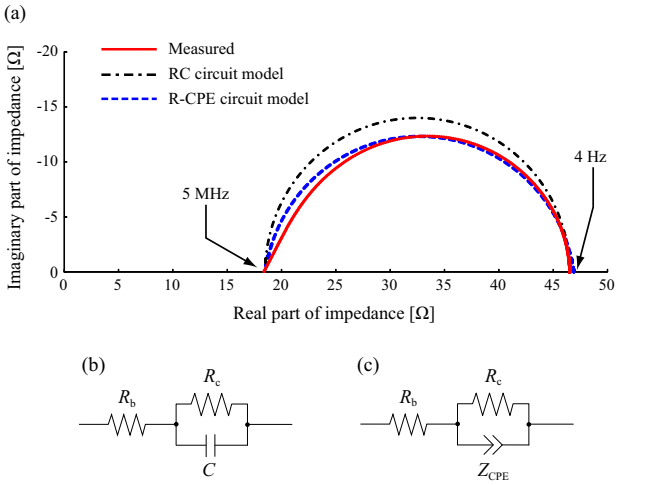

Fig. 7. Complex impedance plot and equivalent circuits. (a) Solid line: complex impedance plot obtained from the two parallel nanowires. Dashed-dotted line: curve fit obtained using the RC circuit model. Dashed line: curve fit obtained using the R-CPE circuit model. (b) Equivalent circuit, assumed to be a series connection of a resistance and a parallel RC circuit. (c) Equivalent circuit, assumed to be a series connection of a resistance and a parallel R-CPE circuit.

Table 1. Parameter values of the RC circuit model and R-CPE circuit model that were used for the fitting curves. X is the CPE coefficient and p is the CPE exponent taking values between 0 and 1. In the cases of $p = 0$ and $p = 1$, the CPE is equivalent to an ideal resistance and an ideal capacitance, respectively.

	R_b [Ω]	R_c [Ω]	C [nF]	X [$\Omega^{-1}s^p$]	p
RC circuit model	18.5	28.0	200	-	-
R-CPE circuit model	18.5	28.0	-	3.0×10^{-7}	0.91

4. Conclusions

We isolated a single λDNA molecule using a nanochannel and formed a single silver nanowire using metallization of the λDNA after it was stretched into a straight strand and immobilized between two electrodes in a nanochannel. Also, we measured the complex impedance of the nanowire and found that a series connection of a resistance and a parallel R-CPE circuit accurately represents the electrical properties of the nanowire. Using this equivalent circuit, the nanowire was found to contain silver grain boundaries, and the total bulk resistance of the two parallel nanowires was estimated to be 18.5 Ω. In this study, we had to estimate the electrical properties of a single nanowire from those of two nanowires. In future work, one of the two electrodes will be divided into 15 portions each of which will be used for one nanochannel. This will allow true electrical evaluation of a single nanowire.

The metallized DNA nanowires which were formed and evaluated in this paper can be applied to electrical detection of biomolecules as follows. The DNA metallization technique using reducing group-labeled intercalator molecules permits double-stranded DNA to be specifically metallized while not permitting metallization of single-stranded DNA. Therefore, partial metallization of DNA complexes consisting of single strands and double strands makes non-metallized portion on metallized DNA nanowires, which gives molecular recognition property to the nanowires. For example, when partially-metallized DNA nanowires are immobilized between two electrodes, deoxyribonuclease (DNase) can be detected by measuring the increase in impedance between the electrodes after DNase cleaves the non-metallized portions of the nanowires.

Acknowledgements

This work was supported by a Grant-in-Aid for Scientific Research (B) (Grant No: 23300168) of JSPS (Japan Society for the Promotion of Science).

References

[1] N. C. Seeman, *Trends Biotechnol.* **1999**, 17, 437-443.

[2] P. W. K. Rothemund, *Nature* **2006**, 440, 297-302.

[3] C. J. Murphy, M. R. Arkin, Y. Jenkins, N. D. Ghatlia, S. H. Bossmann, N. J. Turro, J. K. Barton, *Science* **1993**, 262, 1025-1029.

[4] S. Tuukkanen, A. Kuzyk, J. J. Toppari, V. P. Hytonen, T. Ihalainen, P. Torma, *Appl. Phys. Lett.* **2005**, 87, 183102.

[5] P. Romano, A. Polcari, B. Verruso, V. Colantuoni, W. Saldarriaga, E. Baca, *J. Appl. Phys.* **2007**, 102, 103720.

[6] C. Yamahata, D. Collard, T. Takekawa, M. Kumemura, G. Hashiguchi, H. Fujita, *Biophys. J.* **2008**, 94, 63-70.

[7] T. Tsukamoto, Y. Ishikawa, Y. Sengoku, N. Kurita, *Chem. Phys. Lett.* **2009**, 474, 362-365.

[8] O. Hornack, W. E. Ford, A. Yasuda, J. M. Wessels, *Nano Lett.* **2002**, 2, 919-923.

[9] W. E. Ford, O. Hornack, A. Yasuda, J. M. Wessels, *Adv. Mater.* **2001**, 13, 1793-1797.

[10] E. Braun, Y. Eichen, U. Sivan, G. B. Yoseph, *Nature* **1998**, 391, 775-778.

[11] J. Richter, M. Mertig, W. Pompe, *Appl. Phys. Lett.* **2001**, 78, 536-538.

[12] C. F. Monson, A. T. Woolley, *Nano Lett.* **2003**, 3, 359-363.

[13] J. Richter, R. Seidel, R. Kirsch, M. Mertig, W. Pompe, J. Plaschke, H. K. Schackerl, *Adv. Mater.* **2000**, 12, 507-510.

[14] S. Kundu, H. Liang, *Langmuir* **2008**, 24, 9668-9674.

[15] P. Nickels, W. U. Dittmer, S. Beyer, J. P Kotthaus, F. C. Simmel, *Nanotechnology* **2004**, 15, 1524-1529.

[16] S. M. D. Watson, N. G. Wright, B. R. Horrocks, A. Houlton, *Langmuir* **2010**, 26, 2068-2075.

[17] K. Kobayashi, N. Tonegawa, S. Fujii, J. Hikida, H. Nozoe, K. Tsutsui, Y. Wada, M. Chikira, M. Haga, *Langmuir* **2008**, 24, 13203-13211.

[18] H. A. Becerril, R. M. Stoltenberg, C. F. Monson, A. T. Woolley, *J. Mater. Chem.* **2004**, 14, 611-616.

[19] Y. F. Ma, J. M. Zhang, G. J. Zhang, H. X. He, *J. Am. Chem. Soc.* **2004**, 126, 7097-7101.

[20] S. Pu, A. Zinchenko, S. Murata, *Nanotechnology* **2011**, 22, 375604.

[21] T. Torimoto, M. Yamashita, S. Kuwabata, T. Sakata, H. Mori, H. Yoneyama, *J. Phys. Chem. B* **1999**, 103, 8799-8803.

[22] D. Nyamjav, J. M. Kinsella, A. Ivanisevic, *Appl. Phys. Lett.* **2005**, 86, 093107.

[23] R. Mohammadzadegan, H. Mohabatkar, M. H. Sheikhi, A. Safavi, M. B. Khajouee, *Phys. E* **2008**, 41, 142-145.

[24] K. Ijiro, Y. Matsuo, Y. Hashimoto, *Mol. Cryst. Liq. Cryst.* **2006**, 445, 207-211.

[25] M. Fischler, U. Simon, H. Nir, Y. Eichen, G. A. Burley, J. Gierlich, P. M. E. Gramlich, T. Carell, *Small* **2007**, 3, 1049-1055.

[26] K. Keren, M. Krueger, R. Gilad, G. B. Yoseph, U. Sivan, E. Braun, *Science* **2002**, 297, 72-75.

[27] J. Liu, Y. Geng, E. Pound, S. Gyawali, J. R. Ashton, J. Hickey, A. T. Woolley, J. N. Harb, *ACS Nano* **2011**, 5, 2240-2247.

[28] A. C. Pearson, J. Liu, E. Pound, B. Uprety, A. T. Woolley, R. C. Davis, J. N. Harb, *J. Phys. Chem. B* **2012**, 116, 10551-10560.

[29] S. A. F. Al-Said, R. Hassanien, J. Hannant, M. A. Galindo, S. Pruneanu, A. R. Pike, A. Houlton, B. R. Horrocks, *Electrochem. Commun.* **2009**, 11, 550-553.

[30] K. Komizo, H. Ikedo, S. Sato, S. Takenaka, *Bioconjugate Chem.* **2014**, 25, 1547-1555.

[31] E. Angeli, C. Manneschi, L. Repetto, G. Firpo, U. Valbusa, *Lab Chip* **2011**, 11, 2625-2629.

[32] P. Fanzio, V. Mussi, C. Manneschi, E. Angeli, G. Firpo, L. Repetto, U. Valbusa, *Lab Chip*, **2011**, 11, 2961-2966.

[33] K.-G. Wang, S. Yue, L. Wang, A. Jin, C. Gu, P.-Y. Wang, Y. Feng, Y. Wang, H. Niu, *Microfluid. Nanofluid*. **2006**, 2, 85-88.

[34] J. T. Mannion, C. H. Reccius, J. D. Cross, G. Craighead, *Biophys. J.* **2006**, 90, 4538-4545.

[35] M. Kumemura, D. Collard, C. Yamahata, N. Sakaki, G. Hashiguchi, H. Fujita, *ChemPhysChem* **2007**, 8, 1875-1880.

[36] M. Ueda, H. Iwasaki, O. Kurosawa, M. Washizu, *Jpn. J. Appl. Phys.* **1999**, 38, 2118-2119.

[37] T. Yasui, N. Kaji, R. Ogawa, S. Hashioka, M. Tokeshi, Y. Horiike, Y. Baba, *Anal. Chem.* **2011**, 89, 6635-6640.

[38] T. Yamamoto, T. Fujii, *Nanotechnology* **2010**, 21, 395502.

[39] A. Sadkowski, *J. Electroanal. Chem.* **2000**, 481, 222-226.

[40] A. Sadkowski, *J. Electroanal. Chem.* **2000**, 481, 232-236.

[41] F. Berthier, J.-P. Diard, R. Michel, *J. Electroanal. Chem.* **2001**, 510, 1-11.

[42] J. T. S. Irvine, D. C. Sinclair, A. R. West, *Adv. Mater.* **1990**, 2, 132-138.